Science of the Total Environment 803 (2022) 149963

Contents lists available at ScienceDirect

Science of the Total Environment

journal homepage: www.elsevier.com/locate/scitotenv

GIS-based assessment for the potential of implementation of food-energy-water systems on building rooftops at the urban level

A.L. Montealegre [a,b,1], S. García-Pérez [c,1], S. Guillén-Lambea [a,d], M. Monzón-Chavarrías [c], J. Sierra-Pérez [e,f,*]

[a] Centro Universitario de la Defensa de Zaragoza, Academia General Militar, Ctra. de Huesca s/n, 50090 Zaragoza, Spain
[b] GEOFOREST-IUCA Research Group, Department of Geography, University of Zaragoza, Pedro Cerbuna 12, 50009 Zaragoza, Spain
[c] Department of Architecture, EINA, University of Zaragoza, María de Luna 3, 50018 Zaragoza, Spain
[d] Thermal Engineering and Energy Systems Group (GITSE), Aragón Institute for Engineering Research (I3A), University of Zaragoza, 50018 Zaragoza, Spain
[e] Department of Design and Manufacturing Engineering, EINA, University of Zaragoza, María de Luna 3, 50018 Zaragoza, Spain
[f] Water and Environmental Health-IUCA Research Group, University of Zaragoza, 50018 Zaragoza, Spain

HIGHLIGHTS

- Characterization of building rooftops is performed with LiDAR and Cadastral data.
- Food-Energy-Water (FEW) systems potential depends on urban morphologies.
- Self-production capacity of urban environments can be assessed through FEW potential.
- Industrial and compact residential urban morphologies show the highest potential.

GRAPHICAL ABSTRACT

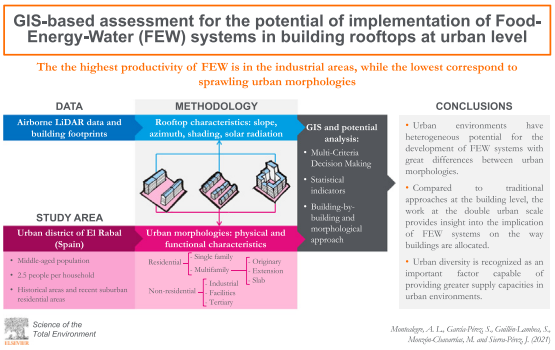

ARTICLE INFO

Article history:
Received 4 May 2021
Received in revised form 20 August 2021
Accepted 23 August 2021
Available online 28 August 2021

Editor: Huu Hao Ngo

Keywords:
LiDAR
Cadastral data
FEW systems
Urban morphology
Urban metabolism
Urban self-sufficiency

ABSTRACT

This research develops a bottom-up procedure to assess the potential of food-energy-water (FEW) systems on the rooftops of buildings in an urban district in Spain considering the urban morphology of the built environment and obtains accurate assessments of production and developmental patterns. A multicriteria decision-making technique implemented in a geographical information system (GIS) environment was used to extract suitable rooftop areas. To implement this method, the slope (tilt), aspect (azimuth), shading, and solar radiation of the rooftops were calculated using LiDAR (Light Detection and Ranging) data and building footprints. The potential of FEW system implementation was analysed at the building and morphology levels. The results showed several differences between residential and non-residential urban morphologies. Industrial areas contained the highest productivity for FEW systems. The production was 2.51 kg of tomatoes/m^2, 48 kWh of photovoltaic energy/m^2, and 0.16 l of rainwater/m^2. Regarding the residential urban morphologies, the more compact tents resulted in better performance. Among the FEW systems, although water could best benefit from the features of the entire roof surface, the best production results were achieved by energy. The food system is less efficient in the built environment since it requires flat roofs. The methodology presented can be applied in any city, and it is considered optimal in the European context for the development of self-production strategies for urban environments.

* Corresponding author at: Department of Design and Manufacturing Engineering, EINA, University of Zaragoza, María de Luna 3, 50018 Zaragoza, Spain.
E-mail addresses: monteale@unizar.es (A.L. Montealegre), sgarciap@unizar.es (S. García-Pérez), sguillen@unizar.es (S. Guillén-Lambea), monzonch@unizar.es (M. Monzón-Chavarrías), jsierra@unizar.es (J. Sierra-Pérez).
[1] These authors contributed equally to this work.

https://doi.org/10.1016/j.scitotenv.2021.149963

1. Introduction

Ensuring good living conditions in cities involves addressing sustainability without compromising the environment, economy and society, especially considering that 68% of the world population is expected to live in urban areas by 2050 (*World Urban. Prospect. 2018 Revis.*, 2019) (European Commission, 2020). It is a fact that the world is transitioning to a predominantly urban world; and irreversible changes in the ways we use land, water, energy and other natural resources are associated with this transition (UN-Habitat, 2010).

This transition places cities at the centre of the climate change agenda because cities already consume 80% of the global energy consumption, generate more than 70% of the total waste and contribute more than 60% of the planet's Greenhouse Gas (GHG) emissions (UN-Habitat, 2010). Therefore, urban sustainability practices are crucial to reduce resource consumption and its impacts (European Environment Agency, 2015), and the transformation towards a circular economy is a great opportunity for cities' sustainability. This approach could address the efficient, close and cyclical design of urban resource systems (Ghisellini et al., 2016). However, there are systems partially outside cities' boundaries, such as food systems; and these systems also contribute to the global environmental performance of citizens (Satterthwaite, 2008).

Most systems, such as food, energy and water, concentrate their consumption at the household level (European Environment Agency, 2015), so the assessment of these systems for addressing circular approaches should be at the same level. In order to effectively handle this scale of work at the urban level, recent research has used so-called building stock aggregation models. Among all the possible building stock aggregation models, this study considers building-by-building approaches as part of bottom-up models (Swan and Ugursal, 2009).

The advantages of using building-by-building approaches have been broadly discussed and include the use of physically measurable data and a higher level of disaggregation. However, these models require a large amount of technical data (Kavgic et al., 2010). The use of Geographic Information Systems (GIS), as well as the open publication and regular updating of much of the data needed to implement these approaches, is becoming more widespread, which make their use highly recommendable.

From an urban metabolism approach, building-by-building approaches have recently been used for two main purposes: the estimation of resource consumption in city boundaries and the estimation of the potential productivity for cities' self-sufficiency.

The estimation of urban resource consumption has been mainly focused on energy and, more specifically, on the building sector. Energy consumption depends on the spatial arrangement, and bottom-up models have been used to estimate the energy consumption of the building stock. For example, in Tuominen et al. (2014), the authors use representative buildings to assess the energy consumption in Finland. Urban energy maps are developed to evaluate the building energy performance in a city or in a district to establish sustainable energy strategies and standards for defining retrofitting scenarios (García-Pérez et al., 2017; Monzón-Chavarrías et al., 2021). Fabbri et al. (2012) used a GIS to evaluate the energy performance indexes for heritage buildings in Ferrara city, Göçer et al. (2016) developed a detailed methodology for retrofitting historical campus buildings, and Johansson et al. (2017) developed an energy atlas of the multifamily building stock in Sweden to analyse energy consumption and determine renovation needs.

Furthermore, the estimation of the urban productivity potential has increasingly focused on building-by-building modeling in the three main resources of urban metabolism: food, energy and water (FEW).

1.1. Food production

Several studies have analysed the potential of cities to host agricultural systems. La Rosa et al. (2014) proposed a method to evaluate the suitability of nonurbanized areas at ground level for transformation into new forms of urban agriculture. These areas were analysed using a combination of GIS and multicriteria decision analysis and considering their proximity to residential areas, their contiguity to farmland, and their tree cover. The characterization of these nonurbanized areas was addressed in terms of their physical, ecological, and social features. This method allowed the proposal of a new land use masterplan that defines a set of new land uses, including urban agriculture.

The combination of GIS and remote sensing data was used to estimate the urban agricultural capacity in Barcelona (Spain) (Nadal et al., 2017) at the rooftop level in non-residential urban areas and in Boston (USA) (Saha and Eckelman, 2017) at the ground and rooftop levels in urban areas. The former study was focused on the use of airborne sensors as data acquisition tools to automatically obtain the area, slope, materials, and solar radiation to install rooftop greenhouses. This data acquisition process was conducted after a study area selection process since these data were not openly available. This previous selection can determine areas with great potential due to the great extension of the metropolitan area (636 km^2). The latter study analysed geospatial information at ground level for vacant public and private lots and underutilized residential and commercial areas considering zones, ownership, slope, soil quality and insolation. This study assumed that the entire available area would be used for urban agriculture but also stated that aspects such as the type of ownership and the economics of small-scale production should be considered later to reflect the real potential more reliably.

1.2. Renewable energy generation

The estimation of the energy production in cities has focused on the installation of solar photovoltaic systems (PVs), which are a mature solution that is easy to install and a clean energy source. Accuracy has improved using GIS methods to assess the electricity potential. Recently, a very remarkable macro study was performed (Bódis et al., 2019) to quantify the available rooftop area for PV systems throughout the European Union (EU), and the results estimated that EU rooftops could potentially produce 24.4% of the energy required to meet current electricity consumption. Many recent studies have evaluated the potential of photovoltaic electricity generation at the regional (Schallenberg-Rodríguez, 2013; Yuan et al., 2016) or country level (Cronemberger et al., 2012; Hong et al., 2014; Izquierdo et al., 2011). The study performed by Gagnon et al. (2016) is notable. They performed a detailed assessment of the potential of PV rooftop installation in the continental United States. Bergamasco and Asinari presented a methodology to estimate the solar energy potential using GIS for the Piedmont region (Italy) (Bergamasco and Asinari, 2011a) and for Turin (Bergamasco and Asinari, 2011b). A city-level approach assuming representative rooftop typologies and empirical coefficients was presented in that study.

With the aim of reducing uncertainties and increasing the accuracy of the assessment of the potential solar energy that can be recovered on rooftops, building-by-building approaches have recently been developed (Amado and Poggi, 2014; Byrne et al., 2015; Hong et al., 2017; Wong et al., 2016). This method has a higher accuracy when analyzing a city or a district in a city because it considers the type of building, the sun position (usually on an hourly basis), the rooftop slope and orientation, and shading effects. Romero Rodríguez et al. (2017), who evaluated the PV potential at the urban scale using 3D city models and processed more than 150,000 buildings, obtained very significant rates of electricity demand covered by PV. However, they did not evaluate the shading effect between buildings, and the literature reviewed showed that a shadowing reduction factor should be considered. Lukac et al. (2013) proposed a new methodology combining LiDAR data, measuring global and diffuse solar irradiances and considering shading to evaluate the solar potential of a roof's surface in the city of Maribor, Slovenia. Nevertheless, the existing bottom-up studies do not aggregate the building stock models.

1.3. Rainwater harvesting

The assessment of the rainwater harvesting potential at the urban level has used bottom-up methodologies to calculate the rainwater harvesting potential in cities and the use of this water for general non-potable uses. Using GIS technology and considering building characteristics, Lúcio et al. (2020) presented a methodology to evaluate the rainwater harvesting potential at an urban level and applied the model to Lisbon, Portugal. Using GIS and LiDAR data, Grant et al. (2018) determined the potential reductions in potable water consumption for households in residential structures of Escambia County, Florida.

Different studies discriminate according to the rainwater collection location. First, some authors have studied the use of rainwater to irrigate urban agriculture on rooftops. Salvador et al. (2019) evaluated the potential of technology parks to become self-sufficient in urban areas using rooftops from the FEW nexus. A study on rooftop greenhouses (Sanjuan-Delmás et al., 2018) analysed the benefits of the synergy between them and buildings in terms of water. Rufí-Salís et al. (2020) demonstrated that between 80 and 90% of rainwater could be used to irrigate crops, and others determined that number to be between 82 and 100%. Other authors studied the rooftop rainwater harvesting potential and the use of the rainwater to irrigate urban agriculture in ground floor gardens in Virginia, USA (Parece et al., 2016) and Rome, Italy (Lupia et al., 2017).

Beyond the partial studies previously discussed, the characterization of FEW potential through a building-by-building approach is an innovative task. Furthermore, relating this approach to morphological data on urban fabrics will allow us to obtain more accurate results to characterise the true potential of our cities (García-Pérez et al., 2018; Oliveira, 2016; Silva et al., 2017). It should be noted that not all urban fabrics have the same physical and functional characteristics (type of roof, average useful area, orientation, shading of urban fabrics, building use, etc.). Therefore, the potential for implementing FEW systems will also be different in different morphologies.

1.4. Objectives

The main objective of this research is to develop a bottom-up procedure to assess the potential installation of FEW systems on rooftops in an urban district of Spain. The study has two specific objectives:

- To assess the potential locations for FEW systems at the building-by-building level based on a multicriteria decision-making procedure using public data and GIS tools.
- To analyse the potential of implementing FEW systems in different urban morphologies according to the physical and functional characteristics.

2. Methodology

In this section, we present an overview of the approach used to estimate the rooftop area that is suitable for the implementation of FEW systems in an urban district. Fig. 1 shows a summary of the study's methodological flow.

Prior to the FEW potential analysis, the study area was selected. Then, LiDAR data and building footprints were processed using GIS methods (Gagnon et al., 2016) in order to determine the slope (tilt), aspect (azimuth), shading, and solar radiation. Subsequently, a set of criteria was applied to select the roof area that is suitable for urban agriculture, photovoltaic deployment, and rainwater harvesting. These results were aggregated at the cadastral reference level (building level), as well as at the urban morphology level, to analyse the suitability of each building rooftop. The following subsections provide the details of each step.

2.1. Study case

The urban district of El Rabal belongs to Zaragoza, the capital city of the autonomous region of Aragón, northeastern Spain (41°39′0″ N, 0°53′0″ W; 208 m.a.s.l.) (Fig. 3). This city lies by the Ebro River, and the climate is Mediterranean-continental. The mean annual air temperature is 14.6 °C (6.2 °C in December and 24.3 °C in July) (Cuadrat Prats, 2004). The mean annual precipitation is 301 mm (concentrated in spring and autumn) with an intense summer drought from June to October (Aragonese Institute of Stadistics, 2010).

In general, this region receives more than 2600 h per year of sunlight, one of the highest numbers of Spain. This is not only due to latitude but also to weak relative humidity values and the low number of days with cloudy skies (Cuadrat Prats, 2004). According to the *Atlas Climático de Aragón* (López Martín et al., 2007), Zaragoza receives 3300-3400 J/m^2/day of potential radiation.

The study area was selected for two main reasons. The first reason is the area's social significance. This district has the second highest percentage of the population and the fourth highest percentage in terms of the area (8.38 km^2) of the urban districts of Zaragoza. Its population, 78,325 inhabitants in 2018, has an average age of 42 years old, and its income is lower than the average income of Zaragoza (Observatorio Urbano de Zaragoza y su Entorno, 2018). The average household size is 2.5 people. The second reason is the area's diversity. El Rabal comprises different urban morphologies, ranging from historical areas to

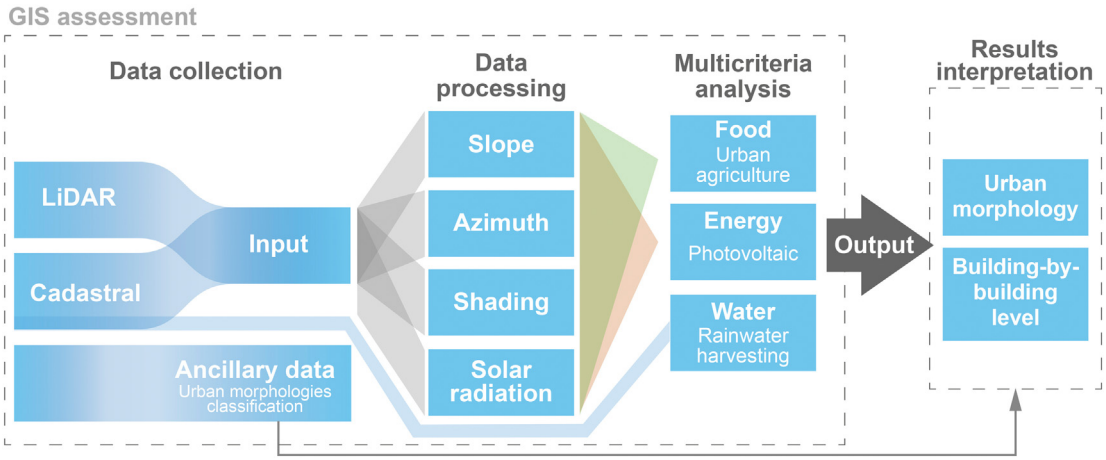

Fig. 1. Conceptual scheme of the proposed methodology.

recent suburban residential ones; and encompasses industrial fabrics whose potential is important to assess.

2.2. Data collection

2.2.1. LiDAR data

In total, six LAS format files of 2 × 2 km were downloaded from the Directorate-General of the National Geographic Institute (IGN) of Spain, and they were combined into one LAS dataset using ArcGIS tools (ESRI). The LiDAR data were captured by the National Plan of Aerial Orthophotography (PNOA) on 15/10/2016 using an airborne Leica ALS80 discrete return sensor. The point density was 1 point/m^2 with a planimetric accuracy of 30 cm and a height accuracy of 20 cm. Since point clouds were classified, those points belonging to classes 7 (noise) and 12 (overlap) were excluded from the analysis to avoid errors.

2.2.2. Cadastral data/building footprint data

The building data of the district were collected from the Spanish Cadastre, which is open for consultation to public administrations, enterprises, and citizens. The building data were provided in shapefile format as polygon geometries or footprints with several attributes, such as cadastral reference (single value per plot), gross floor area, year of construction and uses, among other attributes (Dirección General del Catastro, 2016; Mora-García et al., 2015). Only built areas (i.e., roofs) were selected from other land uses (walkways, green areas or patios) (Izquierdo et al., 2008). In total, 1934 cadastral references, representing 1.8 km^2 of rooftop area, were considered. After grouping the building footprint data according to cadastral reference and height attributes, a 1-metre buffer was applied to the building footprint data. According to Boz et al. (2015) and Martín-Ávila et al. (2016), this helps to remove the noise in LiDAR data since laser returns may not be accurate near roof edges and because roof edges do not support PV panels and food systems (greenhouses).

2.2.3. Ancillary data

The more accurate analysis of the results according to urban morphology requires the classification of urban fabrics. Although these data are open for some cities, in the case of the city of Zaragoza, it was necessary to conduct classification. This process started with land classification from municipal planning (Servicios Técnicos del Ayuntamiento de Zaragoza, 2008), and it considered a recent classification methodology focused on the Spanish context (Vinyes Ballbé et al., 2018). First, the classification considered the use of each plot: residential (R), industrial (I), tertiary (T) or facilities (F). Among the residential areas, a second level can be distinguished between single-family and multifamily plots. Finally, residential morphologies are defined on the basis of their growth patterns and the evolution of the urban fabric.

Specifically, the morphologies considered were the following: (O) Originary fabrics form part of the compact city, and their growth is based on the subdivision of plots of land around the original road networks. Today, these plots have experienced a strong densification process. Depending on their patrimonial and central character, a distinction can be made between (O1) historic and (O2) suburban originary fabrics. Continuing the compact city is the (E1) suburban extension. This is a morphology whose planning gives rise to an ordered road system and a subdivision of plots whose development is focused on the alignment of the streets. The result is a dense and compact perimeter block. A sprawl city is based on slab-like developments. Among the slabs, a first distinction is made between those that form part of unitary organisations but that are not aligned with the street network (S1). This category includes the well-known massive housing estates promoted by post-war urban planning. Another category is represented by unitary organisation slabs aligned to the street network, such as contemporary suburban perimeter blocks (S3). Those slab growths that do not meet these characteristics are considered independent blocks (S2). In this case, only terraced houses have been identified among the single-family morphologies (SF1) (Fig. 2).

2.3. Data processing

First, a digital surface model (DSM) with a 1-metre cell size (Martín Ávila et al., 2016) was created using the first returns of the LiDAR dataset (Bayrakci Boz et al., 2015; Renslow, 2012). The DSM represents the top of the Earth's surface, including buildings, trees and other objects that sit on the terrain (Renslow, 2012). Second, this DSM was the topographic input used to derive the tilt, azimuth, shading and solar radiation of the rooftops. The criteria for classifying the cells of these raster layers were selected according to the FEW system requirements.

2.3.1. Rooftop slope

The steepness of the DSM was calculated using the slope tool from the Spatial Analyst Toolbox. The range of slope values in the output (*Tilt_raster*) is 0° for horizontal roofs to 90° for vertical roofs.

The rooftop slope determines and limits the PV panel tilt angle. The performance of PV panels is strongly affected by the panel position with respect to the sun, and electricity generation is generally highest when the sun incidence angle is perpendicular to the panel. The optimal PV tilt varies depending on the latitude. For higher latitudes, where the sunlight hours in winter are very small compared to the sunlight hours in summer, the optimal PV tilt should be optimized for summer seasons. However, this assumption varies in areas where the sunlight hours in winter are not negligible. In this case, another factor, electricity consumption by season, must be analysed. Moreover, for a fixed latitude, the optimal PV tilt varies from one season to another. All these parameters made the optimization of the panel orientation important especially when the rooftop slope must also be considered. Calculations of the solar radiation on tilted surfaces to estimate the energy produced by the PV modules on a rooftop are very uncommon in the latest publications. Hong et al. (2017) assumed that solar PV panels were installed horizontally with no tilt on entire rooftops. Cronemberger et al. (2012) calculated the optimal tilt in several cities in Brazil, proposing a correlation to calculate the optimal tilt depending on the latitude and concluded that the optimal tilt angle was identical to the city latitude for latitudes higher than 25°. Some authors have calculated the maximum slope for installing PV modules, and the values varied between 40° (Wong et al., 2016) and 60° (Gagnon et al., 2016). The large range variation is due mainly to the latitude of the area where the research is focused (a problem of module performance) and/or PV supplier and installer recommendations (a problem of module installation). Hong et al. (2014) conducted sensitivity analysis depending on the azimuth and the slope of the panels for Seoul and Busan (by region), where the slope varied from 0° to 90°. Gagnon et al. (2016) performed a detailed assessment of the potential of PV rooftop installation in the continental United States. They categorized each rooftop area into 21 orientation classes depending on tilt (four classes plus flat) and azimuth (nine classes). They executed PV simulations using SAM to calculate the thermal performance of a solar installation.

In this study, simulations were made using a PVGIS interactive tool designed to obtain the grid-connected PV performance. The online PVGIS web application (European Commission, 2019), with the present version being PVGIS 5.1, was developed by the European Commission Joint Research Centre; and it calculates the PV module performance depending on several parameters, such as the solar radiation intensity, variations in the solar spectrum, and module temperature. The optimum tilt angle for a PV panel oriented to the south in Zaragoza city is 37°. In this research, the PV panels have a tilt angle equal to the rooftop slope for sloping roofs and 37° for flat roofs (see Section 2.4.2).

2.3.2. Rooftop azimuth

The optimal location and orientation of the modules will be those that maximize the energy captured by the system throughout the

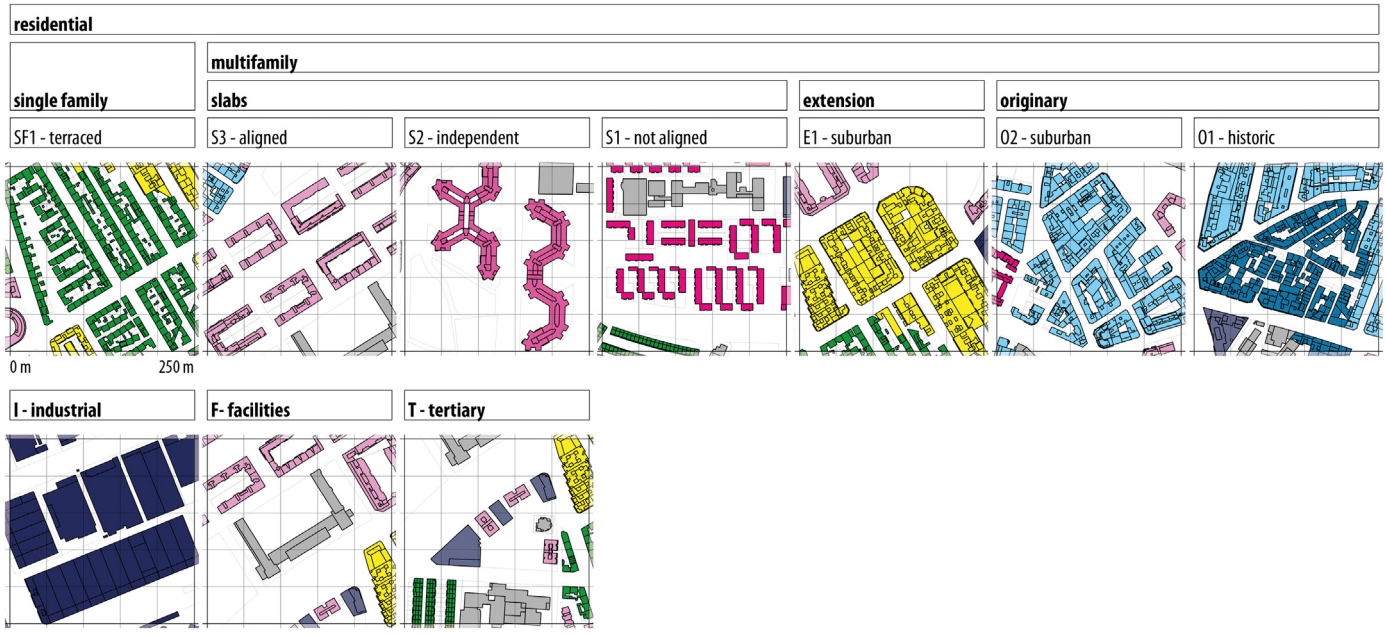

Fig. 2. Urban morphologies of El Rabal (Zaragoza) used for the calculation of the FEW potential.

year. The electric energy to be produced by the PV panels depends on the module orientation: the back azimuth (α), the PV tilt (β) and the latitude (φ). Azimuth indicates the direction in which the slope faces. The aspect tool of the Spatial Analyst Toolbox was used to obtain aspect values from the DSM. The aspect values were measured clockwise in degrees from 0° (due north) to 360° (again due north), coming full circle. Flat areas having no downslope direction are given a value of -1. The resulting aspect layer was converted into "back azimuth" values by subtracting 180 degrees from each cell (*Azimuth_raster*). Thus, 0° represents the south position with positive values to the west and negative values to the east.

The percentage of energy losses due to module orientation and position was calculated according to the Basic Document HE5 of the Spanish Technical Building Code (Instituto para la Diversificación y Ahorro de la Energía, 2009), following Eqs. (1) and (2):

$$\text{If } 15^\circ<\beta<90^\circ, \text{Losses } (\%) = 100 \cdot \left[1.2 \cdot 10^{-4} \cdot (\beta-\phi+10)^2 + 3.5 \cdot 10^{-5} \cdot \alpha^2\right] \quad (1)$$

$$\text{If } \beta\leq 15^\circ, \text{Losses } (\%) = 100 \cdot \left[1.2 \cdot 10^{-4} \cdot (\beta-\phi+10)^2\right] \quad (2)$$

where α is the back azimuth in degrees, β is the tilt in degrees, and ϕ is the latitude.

A rooftop is considered to be suitable for PV system installation if the energy losses due to the tilt and azimuth are less than 20% (Martín Ávila et al., 2016). Both equations were applied using a conditional mapping algebraic expression with the Raster Calculator tool. The result was reclassified into a binary raster (TA_{Losses}_*raster*). The cells with a value greater than 20% were assigned a value of 0 (unsuitable roof), and the cells with a value equal to or below 20% were assigned a value of 1 (suitable roof).

2.3.3. Shading analysis

Shading analysis is an important step for calculating PV potential since shading can significantly reduce power generation. This type of analysis is used to determine the optimal location for PV panels and to ensure sufficient energy production.

Seasonal variation in shading was captured by running the simulation for four days, March 21, June 21, September 21, and December 21, using the Hillshade tool in the Spatial Analyst Toolbox. It should be noted that the shadows cast by structures vary in length and direction throughout the day and between seasons, making it extremely difficult and computationally demanding to perform shading analyses for each day of the year (Bayrakci Boz et al., 2015). This tool requires the altitude and azimuth of the sun as input data. These values were obtained hourly for 2019 from the SoDa (Solar Energy Services for Professionals) web service. Solar Geometry 2 is the second generation of the library for computing the relative position of the sun and the earth made by the MINES ParisTech, and it is valid over the 1980-2030 period. Furthermore, the algorithm is 20 times faster than the SPA (Solar Position Algorithm), with accuracy on the order of approx. 0.005°.

The rooftops suitable for PV installation will be those that are not affected by shadows in the central 4 h of the day throughout the year. The shading analysis was conducted every hour from 10 AM to 2 PM, corresponding to the main sunshine hours. The output raster (*Shading_raster*) ranges from 0, when the shadow are stronger, to 255 when the shadows are weaker. In order to exclude roof cells that were excessively shaded, the *Shading_raster* was reclassified according to Martín Ávila et al. (2016). A new binary raster was defined, $Rec_{Shading}$_*raster*, where all cells with values ranging from 1 to 255 were assigned a value of 1 (no shading and suitable), whereas the rest of the cells remained unchanged, with a value of 0 (shading or no sun and unsuitable).

2.3.4. Solar radiation

Incoming solar radiation (insolation) received from the sun is the primary energy source that drives many of the earth's physical and biological processes. Variations in the slope and aspect and shadows cast by features affect the amount of insolation received at different locations. The solar radiation analysis tools in ArcGIS allow us to map and analyse the effects of the sun over a geographic area for specific time periods based on methods from the hemispherical viewshed algorithm developed by Rich et al. (1994) and Fu and Rich (2002). It should be noted that this model considers climatic features such as atmospheric transmissivity and the proportion of diffuse radiation but does not include radiation reflected from the ground or other surfaces in its calculations (Mangiante et al., 2020). According to Suomalainen et al. (2017), the

ArcGIS Solar Radiation (ASR) tool underestimates the annual solar radiation by approximately 5% on the sunniest spots on the roof, i.e., the most likely spots for eventual solar PV installations. The ASR tool was used to perform insolation analysis for the entire year with monthly intervals for calculations. The output raster represents the total amount of incoming solar insolation (direct and diffuse) calculated for each pixel of the DSM (*Solar_raster*) expressed in watt hours per square metre (Wh/m^2).

2.4. Multicriteria selection: estimation of the available rooftop area

Multicriteria decision analysis using the raster layers created previously to select suitable locations for rooftop greenhouses and solar PV panels was conducted. The desired requirements were summarized in Table 1.

2.4.1. Food: urban agriculture

The type of food production selected in this study is urban agriculture in rooftop greenhouses (RTGs). For this study, tomatoes were selected as the main crop because they are one of the most consumed vegetables in Zaragoza (MercaZaragoza, 2019). The plant density in RTGs was 2 plants/m^2, and the crop productivity in the case of tomatoes was 11.716 kg/m^2 per crop (Rufí-Salís et al., 2020). RTGs use a hydroponic system for irrigation to supply a nutrient solution (water plus fertilisers) (Sanjuan-Delmás et al., 2018) with 64 l of water per kg of tomatoes (Rufí-Salís et al., 2020).

Table 1 shows the production requirements for the implementation of RTGs. The installation of a greenhouse and the required systems requires a load capacity higher than 200 kg/m^2 in a flat roof (surface slope ≤ 10°). The average solar radiation per day during a year was considered, and suitable surfaces received insolation equal to or greater than 3.6 kWh/m^2/day.

2.4.2. Energy: photovoltaic

The annual electricity (E_e obtained in kWh) produced in each rooftop was calculated using Eq. (3) (Wiginton et al., 2010):

$$E_e = I_G \cdot \eta_{PV} \cdot A_{PV} \cdot PR \quad (3)$$

where

I_G is the global annual irradiance in kWh/m^{2}y,
η_{PV} is the PV panel efficiency,
A_{PV} is the area of the installed PV panels in m^2 and
PR is the PV system performance ratio.

The global irradiance (I_G) received for the panels depends on the PV tilt angle. For sloped rooftops (>37°), the panels will be mounted following the rooftop slope, and then the global irradiance is directly obtained from GIS. However, for flat rooftops, the panels should be mounted at the optimal angle for energy production (37°). In this case, the global irradiance obtained from GIS is not the irradiance received for the panel since the global irradiance is not on a flat surface, so an increasing coefficient should be calculated. To estimate this coefficient, simulations were performed using the PVGIS interactive tool designed to obtain the performance of grid-connected PV (European Commission, 2019); accordingly, the panels on flat rooftops should be tilted at 37°, and the increasing coefficient obtained was 1.18 (Table 1).

In order to determine the global irradiance for each rooftop, *Tilt_raster* was reclassified to identify flat and sloped pixels. If the *Tilt_raster* value was greater than 37°, the pixel was assigned a value of 1 ($S_{Coeff}\_raster = 1$); if not, it was assigned a value of 1.18 ($S_{Coeff}\_raster = 1.18$). The global irradiance I_G_raster (I_G in Eq. (3)) is obtained using the Raster Calculator of ArcGIS by multiplying S_{Coeff}_raster by *Solar_raster* expressed in kWh/m^2.

The efficiency of a module (η_{PV}) was assumed to be 16%. Currently, this is a typical value for crystalline silicon modules (Martín Ávila et al., 2016). Polycrystalline modules could have higher values of approximately 17% (Bergamasco and Asinari, 2011b); however, 16% is a very conservative value as the current PV module market is enormously dynamic and the module efficiency announced by manufacturers is increasing.

The system performance ratio (PR) coefficient includes the losses in the system caused by cables, power inverters, dirt, etc. and by the modules because they tend to lose power over the lifetime of the system, depending on the module working conditions and the temperature. The value obtained from PVGIS for this coefficient is 0.79 for flat roofs and 0.76 for sloped roofs. Thus, *Tilt_raster* was reclassified to obtain a new raster with the loss coefficient for each cell (L_{Coeff}_raster). If the slope value was greater than 37°, the pixel value was set as 0.76 (sloped roof); if not, the pixel value was set as 0.79 (flat).

$$PV_{Suitable}\_raster = Rec_{Shading}\_raster \times TA_{Losses}\_raster \quad (4)$$

First, a binary raster, which considers the system losses due to module orientation and the roof area affected by shading, determines if a

Table 1
Summary of the selection criteria for suitable rooftop areas for Food and Energy systems using GIS.

Rooftop characteristic	Raster layer	Values for the food system	Values for the energy system
Slope	*Tilt_raster*: Represents the slope of the rooftop. It ranges from 0° for horizontal roofs to 90° for vertical ones.	0° ≤ *Tilt_raster* ≤ 10°: Flat 10° < *Tilt_raster* ≤ 90°: Sloped	0° ≤ *Tilt_raster* ≤ 37°: Flat. PV tilt angle = 37° 37° < *Tilt_raster* ≤ 90°: Sloped. PV tilt angle = rooftop slope
Azimuth	*Azimuth_raster*: Represents the direction in which the slope of the rooftop faces. 0° indicates the south position, taking positive values to the west until 180°, and negative values to the east until -180°.	–	-180° ≤ *Azimuth_raster* ≤ +180° If Losses ≤ 20%: TALosses_raster = 1 (suitable) If Losses > 20%: TALosses_raster = 0 (unsuitable)
Shading	*Shading_raster*: Represents the shadows according to the Sun's position. It ranges from 0, when the stronger the shadow is, to 255, when the weaker the shadow is.	–	1 ≤ Shading_raster ≤ 255: $Rec_{Shading}$_raster = 1 (suitable) Shading_raster = 0: $Rec_{Shading}$_raster = 0 (unsuitable)
Solar radiation	*Solar_raster* (Wh/m^{2}y): Represents the total amount of incoming solar insolation (direct and diffuse).	0 ≤ *Solar_raster* < 3.6 kWh/m^2/day: Unsuitable *Solar_raster* ≥ 3.6 kWh/m^2/day: Suitable	0 ≤ Tilt_raster ≤ 37°: SCoeff_raster = 1.18 37° < Tilt_raster ≤ 90°: SCoeff_raster = 1 I_G_*raster*: global annual irradiance in kWh/m^{2}y for energy calculation I_G_*raster* = Solar_raster × SCoeff_raster

rooftop is suitable for PV system installation: $PVs_{uitable}\_raster$: 1 (suitable) or 0 (unsuitable) (Eq. (4)).

In order to obtain the real area of the PV panels (A_{PV}), two reduction coefficients of the available area depending on the roof slope should be considered. For sloped roofs (>15°), some free space should be designated for maintenance and access, so a reduction coefficient of 0.95 was applied. No standard value has been found in the literature; and in most publications, no reduction in sloped roofs was considered. Gagnon et al. (2016) used a ratio of 0.98 to reflect just the spacing between each module for clamps, and Ordóñez et al. (2010) determined a percentage of the useful area for pitched roofs (after eliminating the area occupied by other elements) of 0.983 for town houses and 0.789 for high-rise buildings.

For flat roofs (≤15°), the reduction coefficient for PV panels mounted at the optimal tilt angle ($\beta = 37°$) to avoid self-shading was calculated. The value obtained, 0.43, is sufficiently large to assume that the passage areas for maintenance work are guaranteed. It is a very exigent coefficient similar to that applied by other authors such as Byrne et al. (2015) who applied 0.42 for panels at a tilt angle of 30° and Loulas et al. (2012) who used more than 3 m of separation between 30° tilted panels in Thessaloniki, Greece. Gagnon et al. (2016) assumed a ratio of 0.7 for flat roofs to incur only 2.5% losses from self-shading for modules at a 15° tilt.

In the GIS environment, these reduction coefficients were applied as follows. $Available_{Area}\_raster$ represents the available rooftop area in square metres. *Tilt_raster* was reclassified to identify flat and sloped cells. If the slope was greater than 15°, the pixel was assigned a value of 0 (sloped roof); if not, it was assigned a value of 1 (flat roof). This new raster Rec_{tilt}_raster was multiplied by $Available_{Area}\_raster$ to obtain a raster layer only with cell values considered flat rooftops ($Flat_{Available}\_raster$). Next, 1.04 m^2 was the maximum value of the available area of a flat rooftop (≤15°) that was obtained. Therefore, areas equal to or below this value refer to flat roofs, and a reduction coefficient of 0.43 was applied to them. Furthermore, a coefficient of 0.95 was applied to the remaining cells. A conditional mapping algebraic expression with the Raster Calculator tool was executed to obtain A_{PV}_raster. Table 2 shows the parameters used in the GIS model used to estimate the electrical energy obtained by the PV systems.

2.4.3. Water: Rainwater harvesting

Calculating the rainwater harvesting potential can establish the level of self-sufficiency for the irrigation of the agricultural system. To obtain this number, the Zaragoza annual and monthly precipitation in the 1981-2010 period was used (Aragonese Institute of Stadistics, 2010). The entire surface of the rooftops of flat and sloped roofs was considered to determine the water collected, and a 0.8 harvesting efficiency coefficient was applied (Asociación Española de Empresas de Tratamiento y Control de Aguas, 2016; Deutsches Institut fur Normung, 1989; Parece et al., 2016). The potential rooftop rainwater harvesting was calculated for each building using the roof surface that can channel rainwater, the annual precipitation data, and the efficiency coefficient. This rainwater can accumulate in buildings to irrigate food production in RTGs.

2.5. Interpretation of results

Based on the statistical indicators shown in Table 3, the information has been organised on two scales of representation: first, in maps showing the FEW production by building, and second, the production according to the morphological categories. The visualization of the maps was performed using QGIS for the indicators of urban form and FEW described above (Figs. 3 and 4). For each indicator, the centroid of each building, whose size is parametrically related to the assigned value, was represented. In order to visualise the variables homogeneously, each value was rescaled, where the maximum values of each indicator were always represented by the same circle size. The classification based on morphological criteria gives the minimum, maximum, sum and mean for each indicator (Table 4).

3. Results and discussion

3.1. Urban morphologies

The grouping of productivity values according to urban morphology allowed for a discussion of the differences between the fabrics considered in the study. The annual food production, specifically tomatoes, was different depending on the urban form analysed. The highest productivity value was in the industrial area, with 2.51 kg of tomatoes/m^2 of production. This is because most of these buildings have flat roofs with lower gross floor areas. It is important to highlight that these data may be overestimated because the bearing capacity of these buildings should be subsequently analysed for RTG installation, reducing the m^2 availability. In the urban area under study, the average value of the gross floor area of an industrial building was 3645 m^2, so the annual productivity would reach 9 tons of tomatoes per industrial building.

The urban forms with low food productivity are aligned and autonomous blocks; suburban extensions; and originary urban fabrics, both historical and suburban. The values of these urban forms ranged between 0.01 and 0.03 kg of tomatoes/m^2. The conditions for obtaining the food resource were more restrictive than the other two resources analysed in this study. This occurs because in addition to the certain lighting conditions of these urban forms determined by the compactness of the city and the existing shading between buildings, the slope of the roof must be less than 10°. In addition, the most compact urban areas include more buildings with sloping roofs. Assuming an average dwelling of 80 m^2 for these urban forms, for each dwelling, between 0.8 and 2.4 kg of tomatoes per year would be obtained. Knowing that the total consumption of tomatoes in the city is 15.34 kg/capita year (Ministerio de Agricultura Pesca y Alimentación, 2019), the productivity level and the level of self-sufficiency would be low in this type of urban form.

Table 2
Summary of the raster layers and GIS-based multi-criteria decision analysis for electrical energy calculation.

Parameter	Values
E_e (annual electricity in kWh)	$E_e = I_{G}\_raster \cdot 0.16 \cdot A_{PV}\_raster \cdot L_{Coeff}\_raster$ Applied if $PV_{Suitable}\_raster = 1$ $PV_{Suitable}\_raster = Rec_{Shading}\_raster$ x TA_{Losses}_raster (See Table 1)
I_G (global annual irradiance in kWh/m^2y)	$I_{G}\_raster = Solar\_raster \times SCoeff\_raster$ (See Table 1)
η_{PV} (PV panel efficiency)	0.16
A_{PV} (area of the installed PV panels in m^2)	$0 \le Tilt\_raster \le 15°$: $Rec_{tilt}\_raster = 1$ $37° < Tilt\_raster \le 90°$: $Rec_{tilt}\_raster = 0$ $Flat_{Available}\_raster = Rec_{tilt}\_raster$ x $Available_{Area}\_raster$ $A_{PV}\_raster = Con\ (Available_{Area}\_raster \le 1.04, Available_{Area}\_raster \times 0.43, Available_{Area}\_raster \times 0.95)$
PR (PV system performance ratio)	$0 \le Tilt\_raster \le 37°$: $L_{Coeff}\_raster = 0.79$ $37° < Tilt\_raster \le 90°$: $L_{Coeff}\_raster = 0.76$

Table 3
Statistical indicators used to analyse the FEW potential.

Indicator	Description	Formula (Building by building)	Formula (Grouped by urban morphologies)
Voronoi plot area (VPA)	Given the heterogeneity in the drawing of the plot structure, the inefficiency of using the plot surface for morphological analysis has been widely discussed in the literature (Fleischmann et al., 2020). To solve this problem, each plot has been assigned a homogeneously distributed plot area through the Voronoi algorithm, calculated from the centroids of the building, applying an outer buffer of 100 m.	VPA	$\sum VPA$
Roof area (RA)	This considers the horizontal area that a building covers on the ground. It is measured in square metres. To speak in relative terms, the variable 'coverage' has been used, which relates the total roof area to the Voronoi plot area.	RA	$\frac{\sum RA}{\sum VPA}$
Gross floor area (GFA)/Floor area ratio (FAR)	Gross floor area is the total built-up area on a plot of land. It is measured in square metres. If this variable is presented in grouped values, it is used in relative terms. Floor area ratio is then referred to, which relates the gross floor area by the Voronoi plot area.	GFA	$FAR = \frac{\sum GFA}{\sum VPA}$
Energy production (EP)	Energy production, per floor area considers the annual amount of electrical energy (kWh) that a roof can produce through the installation of solar panels, in relation to the gross floor area (m^2).	$EP = \frac{kWh\ per\ year}{GFA}$	$EP = \frac{\sum kWh\ per\ year}{\sum GFA}$
Food production (FP)	Food production, per floor area considers the kilograms of tomatoes (food) produced on a roof annually (kg per year), in relation to the gross floor area (m^2).	$FP = \frac{kg\ per\ year}{GFA}$	$FP = \frac{\sum kg\ per\ year}{\sum GFA}$
Water collection (WC)	Water collection, per built-up area considers the amount of water that a roof can collect annually (m^3 per year), in relation to the gross floor area (m^2).	$WC = \frac{m^3\ per\ year}{GFA}$	$WC = \frac{\sum m^3\ per\ year}{\sum GFA}$

Regarding the remainder of the urban areas with a medium level of productivity, there are two groups of urban forms with different levels of productivity. First, non-residential, equipment and tertiary buildings would produce 0.42 and 0.59 kg of tomatoes/m^2, respectively. This type of urban form could be similar to the industrial type since it includes buildings with mostly flat roofs, although not necessarily with a unique height. The average surface area of these buildings varied from 4000 to 5000 m^2; therefore, the annual productivity of tomatoes would be approximately 2.5 tons per building. Second, residential buildings, nonaligned blocks, and terraced single-family fabrics would produce 0.17 and 0.31 kg of tomatoes/m^2, respectively. These two urban forms had very different characteristics from each other. In addition to their different average living spaces (68 and 267 m^2, respectively), they also differed in whether they were a multifamily or single-family. With these data, the annual production in an average house for these two urban forms would be 5 and 82.7 kg of tomatoes, respectively. The urban form of single-family fabrics would reach high levels of self-sufficiency in the consumption of tomatoes, and it also represented a 20% share in the study area.

As with food production, the generated electrical energy is also strongly affected by the urban form. The highest generation was in the industrial area with an annual electricity generation of 48.09 kWh/m^2. This is mainly due to two reasons. First, industrial buildings are one floor high, and their gross floor area is smaller than that for a block building. Second, most of industrial buildings have flat roofs, and PV panels can be installed at their optimal tilt angle position. Tertiary buildings and facilities generate 13.79 kWh/m^2 and 16.06 kWh/m^2, respectively.

The annual electric energy generated was 4.43 kWh/m^2 and 4.56 kWh/m^2 for autonomous and aligned blocks, respectively; and nonaligned blocks obtained better results, generating up to 8.00 kWh/m^2. The differences were due to the gross floor area of the nonaligned blocks being much smaller since they tend to have lower heights. Terraced single-family fabrics could generate up to 12.81 kWh/m^2 due to their larger available roof area per living space.

The energy consumption of the residential sector in Zaragoza city according to Zaragoza municipality (Ayuntamiento de Zaragoza, 2016) is between 80 and 110 kWh/m^2 for buildings constructed before 1980, 65 kWh/m^2 for buildings erected after 1980 and 25 kWh/m^2 for buildings constructed according to the newest standards. The Spanish Institute for Energy Diversification and Saving – IDAE (Institute for Energy Diversification and Saving - IDAE, 2011) – states that electricity represents 35.1% of the energy consumed in the residential sector, ranging from 28 to 42 kWh/m^2 for buildings erected before 1980 and 23 kWh/m^2 for buildings erected after 1980. Therefore, the electricity that could be generated is not negligible, representing between 17.2% and 26.6% of the consumed electricity for suburban forms, between 14.1% and 21.1% for historical fabrics and between 30.5% and 45.7% for single family fabrics.

Regarding rainwater, the highest potential is the case of industrial fabrics, similar to the case of food and energy. This type of fabric can harvest 0.16 l/m^2 of rainwater. Considering that the average gross floor area of an industrial building is 3645 m^2, the rainwater harvesting potential of industrial buildings is 583.2 l per year. The potential of tertiary buildings and facilities is 0.06 and 0.07 l/m^2, respectively, which, considering the average gross floor area of each type, can achieve 262 and 365 l per year in each respective type of building.

Terraced single-family fabrics have 0.09 l/m^2 of rainwater harvesting supply potential. Considering an average constructed surface of 267 m^2, this type of building can supply 24.03 l per year per home.

The remainder of the urban forms has less supply potential. Aligned and autonomous blocks have a potential of 0.03 l/m^2, and suburban expansions and original expansions have a potential between 0.04 and 0.05 l/m^2. Assuming an average dwelling of 80 m^2, the rainwater harvesting potential is between 2.4 and 4.0 l per dwelling per year. These very low values are due to the small area of the roofs in relation to the number of dwellings and because Zaragoza is a city with low rainfall.

The industrial urban form has six times better capacity and single-family houses have three times better self-sufficiency capacity than autonomous blocks of dwellings. The potential to use roofs for rainwater harvesting is higher than that the potentials for food and energy because there is no restriction by slope or irradiation. Therefore, every building has the potential for rainwater harvesting proportional to the rooftop area. However, the self-sufficiency is very low in the case of multifamily buildings because Zaragoza is a city with low rainfall. The urban form with lower supply levels is autonomous blocks in food, energy and water.

In the urban area studied, the industrial urban form has obtained better self-sufficiency results in food, energy, and water. This is because the rooftop area is high in relation to the built area because these buildings have less gross floor area. Tertiary buildings and facilities have good supply levels because these buildings have between 2 and 4 floors. Single-family houses are dwellings with high levels of self-sufficiency for food, energy, and water; in the case of energy and water use, they are the urban form that ranks second to industrial buildings. In the case of food, single-family houses have good levels but less than tertiary houses and facilities because of their sloped roofs.

3.2. Building by building

Through map visualization, the building-by-building scale makes it possible to illustrate the spatial distribution patterns of FEW productivities. Fig. 4 shows how the distribution is heterogeneous in urban

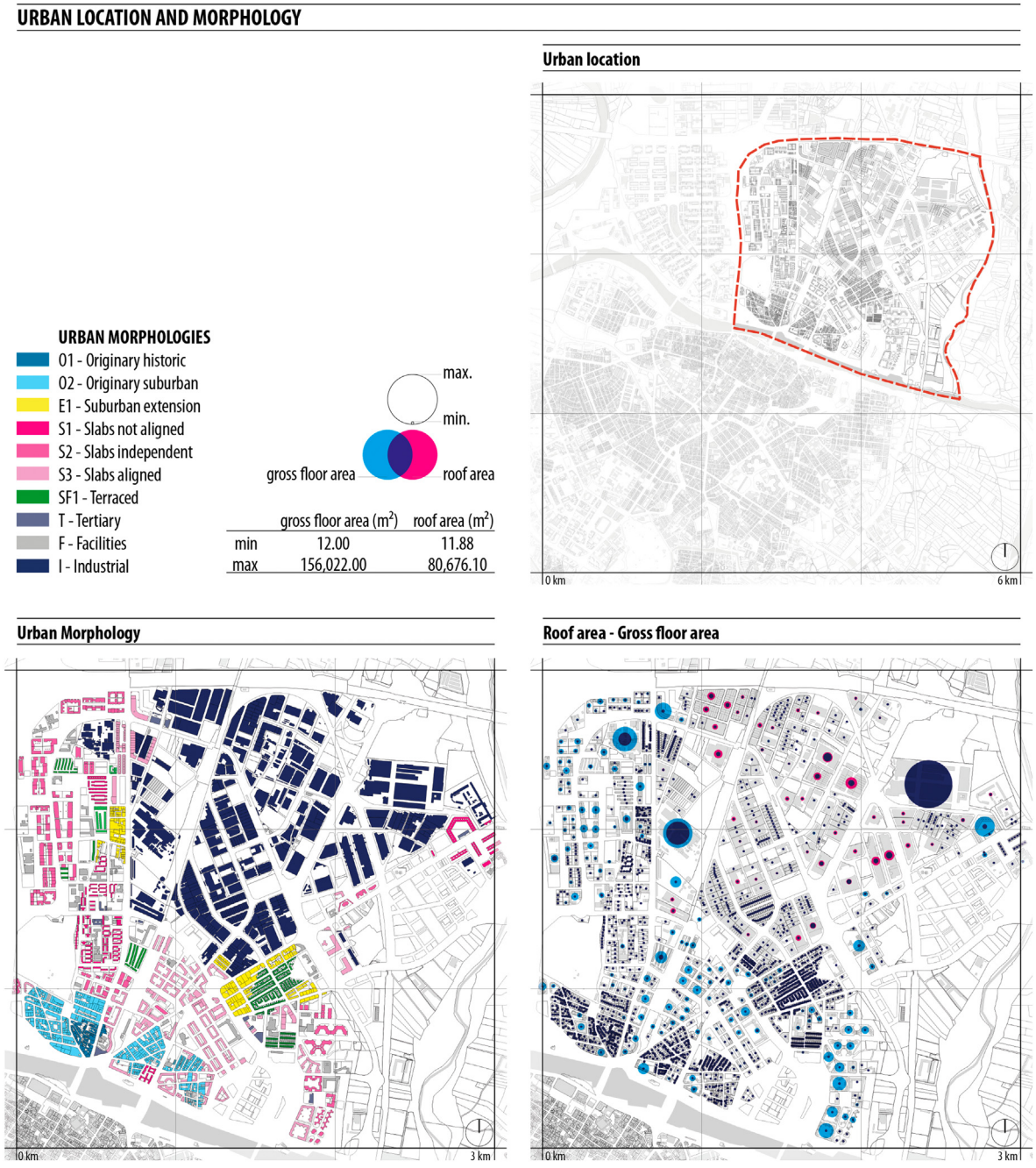

Fig. 3. Urban location, morphology and roof/gross floor area maps.

environments. In contrast to some large production areas, other environments lack supply capacity, at least when considering only the roofs. Industrial areas, located in the upper part of the studied neighbourhood, possess higher productivity. Tertiary and facilities buildings tend to be mixed between residential urban forms. Regarding the residential forms, the more compact fabrics and the terraced single-family fabric achieve better results because they are more grouped together and therefore have larger roof surfaces with a larger gross floor area. The more sprawled fabrics do not have as much potential over the territory because they have much less roof area for the same or an even larger floor area. In these cases, considering the value of the land (and not just the roof) can be key to increasing self-production. The food variable differs slightly from these spatial patterns as it is highly dependent on the existence of flat roofs.

3.3. Comparison with previous research and methodological limitations

As noted in the Introduction section, the majority of the existing literature was focused on the evaluation/estimation of the current and/or future resource consumption regarding the physical and metabolic characteristics of cities. The proposed methodology incorporates the need to respond to this growing consumption in cities with a strategy such as self-sufficiency and that the city is a producer of its own resources. This does not achieve total self-sufficiency, but it can alleviate the consequences of this growth.

The results of this research cannot be directly compared with the results obtained from other research. First, the results strongly depend on the urban morphologies of the city under study (great dependence on the type of building exists in the results), in addition to the methodology

Fig. 4. Building-by-building production maps for FEW systems.

used to calculate the top roof area available, the position and efficiency of the photovoltaic panels, rainfall rates, and the solar radiation, among other factors. In addition, the FEW consumption of a city varies strongly throughout the world not only due to climatic conditions but also because consumption habits vary greatly from one country to another.

The proposed methodology has some strengths compared to other studies. For example, we consider urban forms in the FEW potential analysis of an urban district to understand the diverse behaviour of the built environment, considering the shadow effect to provide more accurate results (Saha and Eckelman, 2017), and the cadastral data used are of high quality in terms of the geometry and functional parameters (Lupia et al., 2017).

However, the methodology presented has some limitations. It should be noted that the assumptions used are simplifications of a complex urban reality. This study does not consider the ability to install FEW systems and only considers the harvesting potentials. All rooftops have been considered regardless of their functionality, such as penthouses with terraces. Moreover, buildings have physical limitations. For example, the bearing capacity, materials and pavement of the roof can influence the installation of FEW systems (Nadal et al., 2017). In order to better describe building rooftops, a higher LiDAR point density is necessary. The use of high spatial resolution optical images or hyperspectral data could help to identify structural elements or roof covering materials (metal roofing, asphalt shingle roofing, clay, or concrete tiles, etc.) unsuitable for FEW systems. Especially for greenhouses, it is necessary to know the type of rooftop access since it must be comfortable and safe and the common spaces in the case of multifamily buildings. If the necessary conditions do not exist, rooftop retrofitting may not be economically or technically feasible. This study uses an urban approach, which makes it difficult to know the specific state of all buildings and

Table 4
Urban morphology production values for FEW systems. O1 - Originary historic; O2 - Originary suburban; E1 - Suburban extension; S1 - Slab not aligned; S2 - Slab independent; S3 - Slab aligned; SF1 – Single- Family terraced; T – Tertiary; F – Facilities; I – Industrial; UMR-Uban morphology representativeness.

		Residential morphologies							Non-residential morphologies		
		O1	O2	E1	S1	S2	S3	SF1	T	F	I
	n° plots	106	413	181	131	122	161	359	14	67	380
	UMR (%)	5,48	21,35	9,36	6,77	6,31	8,32	18,56	0,72	3,46	19,65
Voronoi plot área (m^2)	sum	55,192.32	400,468.77	228,837.91	527,230.10	1,174,860.93	853,490.29	166,873.79	89,514.79	706,242.90	3,319,403.96
	avg	520.68	969.66	1264.30	4024.66	9630.01	5301.18	464.83	6393.91	10,540.94	8735.27
	min	86.41	99.34	125.20	393.52	1153.66	376.64	138.72	1645.97	523.61	267.14
	max	16,538.50	19,746.37	22,048.94	165,803.81	180,354.61	33,593.87	14,328.56	15,706.69	60,759.21	370,468.59
Roof área (m^2)	sum	19,072.29	127,282.72	78,449.15	58,912.50	142,038.48	167,552.82	49,932.11	16,253.39	101,131.46	948,294.36
	avg	179.93	308.19	433.42	449.71	1164.25	1040.70	139.09	1160.96	1509.42	2495.51
	min	11.89	12.66	63.27	35.63	236.88	92.71	25.17	234.78	16.49	62.76
	max	903.08	3244.71	3620.34	7766.92	4540.91	5696.13	8023.39	2659.40	7633.68	80,676.10
Coverage (%)	sum	0.35	0.32	0.34	0.11	0.12	0.20	0.30	0.18	0.14	0.29
	avg	0.55	0.49	0.49	0.21	0.20	0.28	0.36	0.25	0.25	0.53
	min	0.02	0.00	0.01	0.00	0.01	0.01	0.01	0.04	0.02	0.01
	max	2.45	2.05	1.44	1.08	0.51	0.92	0.82	0.67	2.85	1.81
Gross floor area (m^2)	sum	96,517.00	628,132.00	485,331.00	347,532.00	1,247,782.00	1,421,676.00	132,687.00	61,129.00	349,233.00	1,385,325.00
	avg	910.54	1520.90	2681.39	2652.92	10,227.72	8830.29	369.60	4366.36	5212.43	3645.59
	min	12.00	12.00	76.00	36.00	548.00	186.00	26.00	233.00	17.00	45.00
	max	6979.00	23,126.00	15,075.00	65,378.00	44,614.00	54,830.00	39,427.00	16,768.00	24,639.00	156,022.00
Floor area ratio (m^2/m^2)	sum	1.75	1.57	2.12	0.66	1.06	1.67	0.80	0.68	0.49	0.42
	avg	2.38	2.00	2.52	1.17	1.73	2.11	0.72	0.78	0.75	0.67
	min	0.02	0.00	0.05	0.00	0.03	0.11	0.03	0.04	0.02	0.01
	max	13.45	9.57	10.38	9.05	6.07	9.24	2.75	2.80	8.22	4.38
Energy production (kWh/m^2 y)	sum	5.92	7.45	6.03	8.00	4.44	4.56	12.81	13.79	16.06	48.09
	avg	7.68	11.10	10.60	9.37	5.06	5.97	20.10	23.31	22.89	56.51
	min	0.00	1.50	0.47	2.19	1.79	1.70	0.36	5.04	0.00	1.48
	max	28.35	63.88	92.32	65.86	39.96	56.40	77.32	48.16	71.76	151.90
Food production (kg/m^2 y)	sum	0.01	0.03	0.03	0.17	0.01	0.03	0.31	0.59	0.42	2.51
	avg	0.03	0.07	0.08	0.31	0.02	0.04	0.20	1.55	0.90	2.31
	min	0.00	0.00	0.00	0.00	0.00	0.00	0.00	0.00	0.00	0.00
	max	0.44	3.19	1.74	8.98	1.24	1.13	2.05	7.61	8.08	19.05
Water collection (m^3/m^2 y)	sum	0.05	0.05	0.04	0.04	0.03	0.03	0.09	0.06	0.07	0.16
	avg	0.07	0.08	0.07	0.05	0.03	0.04	0.16	0.12	0.11	0.20
	min	0.02	0.02	0.02	0.02	0.01	0.02	0.05	0.03	0.01	0.01
	max	0.24	0.29	0.25	0.24	0.24	0.25	0.27	0.24	0.26	0.50

their special characteristics to determine the constructive feasibility of the installation of roof production infrastructures.

Regarding the multicriteria analysis, the selection of the type of crop, in this case tomatoes, conditioned the results. As mentioned, this selection was based on the existing demand for tomatoes in the study area and the possibility of being grown hydroponically over an eight-month period due to the tomato cultivation season. However, multiple crops and different vegetables could extend the cultivation season to the entire year. In addition, data on the productivity of tomatoes in greenhouses under cover have been extracted from studies conducted in nearby areas; however, due to the slightly different climatic conditions, the results could vary.

With regard to electrical energy, it seems that the values obtained are estimated to be slightly lower due to the ArcGIS solar radiation method and because of the fairly demanding methodology applied when accounting for the available rooftop areas, orientation solar losses, shadows and separation between PV panels. These considerations lead to the limitation that the estimations of the energy potential that could be generated should still be higher than those obtained in this study.

To estimate the potential for water self-sufficiency, rooftop rainwater harvesting was calculated, but the storage spaces in the building were not studied. Water could be stored in tanks on flat rooftops if there is sufficient space and the roofs have adequate bearing capacities. Otherwise, water could be stored inside the building, even in the basement, but it would be necessary to install pumps to bring the water up to the roof to irrigate crops.

4. Conclusions

This study presents a methodology for Food-Energy-Water (FEW) potential assessment through the evaluation of the roof surface available for growing tomatoes, for roof-top integrated PV systems, and for collecting rainwater. This procedure, based on geographic information systems, requires the definition of a set of criteria that surfaces should meet using freely accessible data, such as LiDAR point clouds and cadastral data of the study area, which makes it reproducible for other cities depending on the computational resources available.

In the present work, the methodology was applied to the urban district of El Rabal (Zaragoza, northeastern Spain). Different indicators have been used to calculate the FEW potential at the building level and at the morphological level grouped into residential, tertiary, facility, and industrial buildings.

First, from non-residential morphologies, industrial areas have the highest food (2.51 kg of tomatoes/m^2), energy (48.09 kWh/m^2/year) and water (0.16 l/m^2 of rainwater) potentials. Second, the single-family terraced morphology presented the highest potential for FEW systems, reaching 0.31 kg of tomatoes/m^2, 12.81 kWh/m^2/year of solar energy, and 0.09 l/m^2 of rainwater. These results confirm that European cities have heterogeneous potential for the development of FEW systems with great differences between urban morphologies. Building-by-building production maps have shown the heterogeneity of the urban environment analysed. This double approach is essential when proposing building transformation strategies since the FEW potential is determined not only by the characteristics of the building but also by its intensity in the built environment. In fact, urban diversity is recognized as an important factor capable of providing greater supply capacities in urban environments.

Despite the identified limitations of the methodology, this study remarks on the capacity of rooftops as a source of food-energy-water production at the urban scale and opens a line of research on the self-production capacities of urban environments. For example, a future

line of work could evaluate the combined installation of greenhouses, photovoltaic panels and water tanks to achieve a totally green strategy in renewable energy exploitation. By identifying the morphologies of the suitable areas with different production potentials or even combining FEW potential layers in a GIS with socioeconomic data, stakeholders and policymakers can be encouraged to discover, design and develop new systems capable of responding to FEW needs in proximity or new distribution networks for these services.

Funding sources

Research supported by the Universidad de Zaragoza under project UZ2020-TEC-07. No funding source governed the design, data collection and interpretation of this article.

CRediT authorship contribution statement

A.L. Montealegre: Methodology, Formal analysis, Investigation, Data curation, Writing – original draft, Visualization. **S. García-Pérez:** Methodology, Formal analysis, Investigation, Data curation, Writing – original draft, Visualization. **S. Guillén-Lambea:** Methodology, Investigation, Data curation, Writing – original draft. **M. Monzón-Chavarrías:** Methodology, Investigation, Data curation, Writing – original draft. **J. Sierra-Pérez:** Conceptualization, Methodology, Writing – review & editing, Supervision, Project administration, Funding acquisition.

Declaration of competing interest

The authors declare that they have no known competing financial interests or personal relationships that could have appeared to influence the work reported in this paper.

References

Asociación Española de Empresas de Tratamiento y Control de Aguas, 2016. Guía técnica de aprovechamiento de aguas pluviales en edificios.

Amado, M., Poggi, F., 2014. Solar urban planning: a parametric approach. Energy Procedia 48, 1539–1548. https://doi.org/10.1016/j.egypro.2014.02.174.

Aragonese Institute of Stadistics, 2010. Usual monthly and annual precipitation values by countries, municipalities and measuring stations. Period 1981-2010. Aragón.

Ayuntamiento de Zaragoza, 2016. Rendimiento energético. 11.

Bayrakci Boz, M., Calvert, K., Brownson, R.S., J., 2015. An automated model for rooftop PV systems assessment in ArcGIS using LIDAR. AIMS Energy 3, 401–420. https://doi.org/10.3934/energy.2015.3.401.

Bergamasco, L., Asinari, P., 2011a. Scalable methodology for the photovoltaic solar energy potential assessment based on available roof surface area: application to Piedmont region (Italy). Sol. Energy 85, 1041–1055. https://doi.org/10.1016/j.solener.2011.02.022.

Bergamasco, L., Asinari, P., 2011b. Scalable methodology for the photovoltaic solar energy potential assessment based on available roof surface area: further improvements by ortho-image analysis and application to Turin (Italy). Sol. Energy 85, 2741–2756. https://doi.org/10.1016/j.solener.2011.08.010.

Bódis, K., Kougias, I., Jäger-Waldau, A., Taylor, N., Szabó, S., 2019. A high-resolution geospatial assessment of the rooftop solar photovoltaic potential in the European Union. Renew. Sust. Energ. Rev. 114, 109309. https://doi.org/10.1016/j.rser.2019.109309.

Byrne, J., Taminiau, J., Kurdgelashvili, L., Kim, K.N., 2015. A review of the solar city concept and methods to assess rooftop solar electric potential, with an illustrative application to the city of Seoul. Renew. Sust. Energ. Rev. 41, 830–844. https://doi.org/10.1016/j.rser.2014.08.023.

Cronemberger, J., Caamaño-Martín, E., Sánchez, S.V., 2012. Assessing the solar irradiation potential for solar photovoltaic applications in buildings at low latitudes - making the case for Brazil. Energy Build. 55, 264–272. https://doi.org/10.1016/j.enbuild.2012.08.044.

Cuadrat Prats, J.M., 2004. El clima de Aragón. In: Peña, J.L., Longares, L.A., Sánchez, M. (Eds.), Geografía Física de Aragón (Aspectos Generales y Temáticos). IFC-Universidad de Zaragoza, Dpto. de Geografía y Ordenación del Territorio, Zaragoza (Spain), p. 12.

Deutsches Institut fur Normung, 1989. Norma DIN 1989-1:2001-10. Regenwassernutzungsanlagen-Teil 1: Planung, Ausführung, Betrieb und Wartung.

Dirección General del Catastro, 2016. Cartografía Catastral Urbana [WWW Document].

European Commission, 2020. New Leipzig Charter- The Transformative Power of Cities for the Common Good.

European Commission, J.R.C, 2019. Photovoltaic Geographical Information System (PVGIS).

European Environment Agency, 2015. Urban Sustainability Issues — What is a Resource-efficient City?, Urban Sustainability Issues — What is a Resource-efficient City? https://doi.org/10.2800/389017

Fabbri, K., Zuppiroli, M., Ambrogio, K., 2012. Heritage buildings and energy performance: mapping with GIS tools. Energy Build. 48, 137–145. https://doi.org/10.1016/j.enbuild.2012.01.018.

Fleischmann, M., Feliciotti, A., Romice, O., Porta, S., 2020. Morphological tessellation as a way of partitioning space: improving consistency in urban morphology at the plot scale. Comput. Environ. Urban. Syst. 80, 101441. https://doi.org/10.1016/j.compenvurbsys.2019.101441.

Fu, P., Rich, P.M., 2002. A geometric solar radiation model with applications in agriculture and forestry. Comput. Electron. Agric. 37, 25–35. https://doi.org/10.1016/S0168-1699(02)00115-1.

Gagnon, Pieter, Margolis, Robert, Melius, Jennifer, Phillips, Caleb, Elmore, Ryan, 2016. Rooftop Solar Photovoltaic Technical Potential in the United States: A Detailed Assessment. Golden (USA).

García-Pérez, S., Sierra-Pérez, J., Boschmonart-Rives, J., Lladó Morales, G., Romero Cálix, A., 2017. A characterisation and evaluation of urban areas from an energy efficiency approach, using geographic information systems in combination with life cycle assessment methodology. Int. J. Sustain. Dev. Plan. 12, 294–303. https://doi.org/10.2495/SDP-V12-N2-294-303.

García-Pérez, S., Sierra-Pérez, J., Boschmonart-Rives, J., 2018. Environmental assessment at the urban level combining LCA-GIS methodologies: a case study of energy retrofits in the Barcelona metropolitan area. Build. Environ. 134C, 191–204. https://doi.org/10.1016/j.buildenv.2018.01.041.

Ghisellini, P., Cialani, C., Ulgiati, S., 2016. A review on circular economy: the expected transition to a balanced interplay of environmental and economic systems. J. Clean. Prod.. https://doi.org/10.1016/j.jclepro.2015.09.007.

Göçer, Ö., Hua, Y., Göçer, K., 2016. A BIM-GIS integrated pre-retrofit model for building data mapping. Build. Simul. 9, 513–527. https://doi.org/10.1007/s12273-016-0293-4.

Grant, A.T.J., McKinney, N.L., Ries, R., 2018. An approach to quantifying rainwater harvesting potential using imagery, geographic information systems (GIS) and LiDAR data. Water Supply 18, 108–118. https://doi.org/10.2166/ws.2017.026.

Hong, T., Koo, C., Park, J., Park, H.S., 2014. A GIS (geographic information system)-based optimization model for estimating the electricity generation of the rooftop PV (photovoltaic) system. Energy 65, 190–199. https://doi.org/10.1016/j.energy.2013.11.082.

Hong, T., Lee, M., Koo, C., Jeong, K., Kim, J., 2017. Development of a method for estimating the rooftop solar photovoltaic (PV) potential by analyzing the available rooftop area using hillshade analysis. Appl. Energy 194, 320–332. https://doi.org/10.1016/j.apenergy.2016.07.001.

Institute for Energy Diversification and Saving - IDAE, 2011. Project Sech-Spahousec, Analysis of the Energetic Consumption of the Residential Sector in Spain (Proyecto Sech-Spahousec, Análisis del consumo energético del sector residencial en España). Idae, p. 76.

Instituto para la Diversificación y Ahorro de la Energía, 2009. Sección HE 5 Contribución fotovoltaica mínima de energía eléctrica. Doc. Básico HE Ahorr. Energía, pp. 1–17.

Izquierdo, S., Rodrigues, M., Fueyo, N., 2008. A method for estimating the geographical distribution of the available roof surface area for large-scale photovoltaic energy-potential evaluations. Sol. Energy 82, 929–939. https://doi.org/10.1016/j.solener.2008.03.007.

Izquierdo, S., Montañés, C., Dopazo, C., Fueyo, N., 2011. Roof-top solar energy potential under performance-based building energy codes: the case of Spain. Sol. Energy 85, 208–213. https://doi.org/10.1016/j.solener.2010.11.003.

Johansson, T., Olofsson, T., Mangold, M., 2017. Development of an energy atlas for renovation of the multifamily building stock in Sweden. Appl. Energy 203, 723–736. https://doi.org/10.1016/j.apenergy.2017.06.027.

Kavgic, M., Mavrogianni, A., Mumovic, D., Summerfield, A., Stevanovic, Z., Djurovic-Petrovic, M., 2010. A review of bottom-up building stock models for energy consumption in the residential sector. Build. Environ. 45, 1683–1697. https://doi.org/10.1016/j.buildenv.2010.01.021.

La Rosa, D., Barbarossa, L., Privitera, R., Martinico, F., 2014. Agriculture and the city: a method for sustainable planning of new forms of agriculture in urban contexts. Land Use Policy 41, 290–303. https://doi.org/10.1016/j.landusepol.2014.06.014.

López Martín, F., Millet Cabrera, M., Cuadrat Prats, J.M., 2007. Atlas climático de Aragón. Diputación General de Aragón, Zaragoza (Spain).

Loulas, N.M., Karteris, M.M., Pilavachi, P.A., Papadopoulos, A.M., 2012. Photovoltaics in urban environment: a case study for typical apartment buildings in Greece. Renew. Energy 48, 453–463. https://doi.org/10.1016/j.renene.2012.06.009.

Lúcio, C., Silva, C.M., Sousa, V., 2020. A scale-adaptive method for urban rainwater harvesting simulation. Environ. Sci. Pollut. Res. 27, 4557–4570. https://doi.org/10.1007/s11356-019-04889-6.

Lukac, N., Žlaus, D., Seme, S., Žalik, B., Štumberger, G., 2013. Rating of roofs' surfaces regarding their solar potential and suitability for PV systems, based on LiDAR data. Appl. Energy 102, 803–812. https://doi.org/10.1016/j.apenergy.2012.08.042.

Lupia, F., Baiocchi, V., Lelo, K., Pulighe, G., 2017. Exploring rooftop rainwater harvesting potential for food production in urban areas. Agriculture 7, 46. https://doi.org/10.3390/agriculture7060046.

Mangiante, M.J., Whung, P.Y., Zhou, L., Porter, R., Cepada, A., Campirano, E., Licon, D., Lawrence, R., Torres, M., 2020. Economic and technical assessment of rooftop solar photovoltaic potential in Brownsville, Texas, U.S.A. Comput. Environ. Urban Syst. 80, 101450. https://doi.org/10.1016/j.compenvurbsys.2019.101450.

Martín Ávila, A.M., Domínguez Bravo, J., Amador Guerra, J., 2016. Desarrollo de un Modelo GEOGRÁFICO Para la EVALUACIÓN del potencial fotovoltaico en entornos urbanos. GeoFocus. Rev. Int. Cienc. y Tecnol. la Inf. Geográfica. 18. https://doi.org/10.21138/GF.483.

MercaZaragoza, 2019. Informe Anual 2018. Zaragoza (Spain).

Ministerio de Agricultura Pesca y Alimentación, 2019. INFORME DEL CONSUMO ALIMENTARIO EN ESPAÑA 2018. Madrid.
Monzón-Chavarrías, M., Guillén-Lambea, S., García-Pérez, S., Montealegre-Gracia, A.L., Sierra-Pérez, J., 2021. Heating energy consumption and environmental implications due to the change in daily habits in residential buildings derived from COVID-19 crisis: the case of Barcelona, Spain. Sustainability 13, 918. https://doi.org/10.3390/su13020918.
Mora-García, R.T., Céspedes-López, M.F., Pérez-Sánchez, J.C., Pérez-Sánchez, V.R., 2015. Reutilización de datos catastrales para estudios urbanos. In: de la Riva, J., Ibarra, P., Montorio, R., Rodrigues, M. (Eds.), Análisis Espacial y Representación Geográfica: Innovación y Aplicación. Universidad de Zaragoza - AGE, pp. 295–304.
Nadal, A., Alamús, R., Pipia, L., Ruiz, A., Corbera, J., Cuerva, E., Rieradevall, J., Josa, A., 2017. Urban planning and agriculture. methodology for assessing rooftop greenhouse potential of non-residential areas using airborne sensors. Sci. Total Environ. 601–602, 493–507. https://doi.org/10.1016/j.scitotenv.2017.03.214.
Observatorio Urbano de Zaragoza y su Entorno, 2018. Zaragoza en datos. Informe global sobre la ciudad y sus distritos. Zaragoza (Spain).
Oliveira, V., 2016. Urban morphology. The Urban Book Series. Springer International Publishing, Cham https://doi.org/10.1007/978-3-319-32083-0.
Ordóñez, J., Jadraque, E., Alegre, J., Martínez, G., 2010. Analysis of the photovoltaic solar energy capacity of residential rooftops in Andalusia (Spain). Renew. Sust. Energ. Rev. 14, 2122–2130. https://doi.org/10.1016/j.rser.2010.01.001.
Parece, T.E., Lumpkin, M., Campbell, J.B., 2016. Irrigating Urban Agriculture With Harvested Rainwater: Case Study in Roanoke, Virginia, USA, pp. 235–263 https://doi.org/10.1007/978-3-319-29337-0_8.
Renslow, M., 2012. Manual of airborne topographic LiDAR. Imaging and Geospatial Information Society, Bethesda, Maryland.
Rich, P.M., Dubayah, R., Hetrick, W.A., Saving, S.C., 1994. Using viewshed models to calculate intercepted solar radiation: applications in ecology. Am. Soc. Photogramm. Remote Sens. Tech. Pap, 524–529.
Romero Rodríguez, L., Duminil, E., Sánchez Ramos, J., Eicker, U., 2017. Assessment of the photovoltaic potential at urban level based on 3D city models: a case study and new methodological approach. Sol. Energy 146, 264–275. https://doi.org/10.1016/j.solener.2017.02.043.
Rufí-Salís, M., Petit-Boix, A., Villalba, G., Ercilla-Montserrat, M., Sanjuan-Delmás, D., Parada, F., Arcas, V., Muñoz-Liesa, J., Gabarrell, X., 2020. Identifying eco-efficient year-round crop combinations for rooftop greenhouse agriculture. Int. J. Life Cycle Assess. 25, 564–576. https://doi.org/10.1007/s11367-019-01724-5.
Saha, M., Eckelman, M.J., 2017. Growing fresh fruits and vegetables in an urban landscape: a geospatial assessment of ground level and rooftop urban agriculture potential in Boston, USA. Landsc. Urban Plan. 165, 130–141. https://doi.org/10.1016/J.LANDURBPLAN.2017.04.015.
Salvador, D.S., Toboso-Chavero, S., Nadal, A., Gabarrell, X., Rieradevall, J., da Silva, R.S., 2019. Potential of technology parks to implement roof mosaic in Brazil. J. Clean. Prod. 235, 166–177. https://doi.org/10.1016/J.JCLEPRO.2019.06.214.
Sanjuan-Delmás, D., Llorach-Massana, P., Nadal, A., Ercilla-Montserrat, M., Muñoz, P., Montero, J.I., Josa, A., Gabarrell, X., Rieradevall, J., 2018. Environmental assessment of an integrated rooftop greenhouse for food production in cities. J. Clean. Prod. 177, 326–337. https://doi.org/10.1016/j.jclepro.2017.12.147.
Satterthwaite, D., 2008. Cities' contribution to global warming: notes on the allocation of greenhouse gas emissions. Environ. Urban.. https://doi.org/10.1177/0956247808096127.
Schallenberg-Rodríguez, J., 2013. Photovoltaic techno-economical potential on roofs in regions and islands: the case of the Canary Islands. methodological review and methodology proposal. Renew. Sust. Energ. Rev. 20, 219–239. https://doi.org/10.1016/j.rser.2012.11.078.
Servicios Técnicos del Ayuntamiento de Zaragoza, 2008. Texto refundido del plan general de Ordenación Urbana de diciembre de 2007.
Silva, M., Oliveira, V., Leal, V., 2017. Urban form and energy demand. J. Plan. Lit. 32, 346–365. https://doi.org/10.1177/0885412217706900.
Suomalainen, K., Wang, V., Sharp, B., 2017. Rooftop solar potential based on LiDAR data: bottom-up assessment at neighbourhood level. Renew. Energy 111, 463–475. https://doi.org/10.1016/j.renene.2017.04.025.
Swan, L.G., Ugursal, V.I., 2009. Modeling of end-use energy consumption in the residential sector: a review of modeling techniques. Renew. Sust. Energ. Rev. 13, 1819–1835. https://doi.org/10.1016/j.rser.2008.09.033.
Tuominen, P., Holopainen, R., Eskola, L., Jokisalo, J., Airaksinen, M., 2014. Calculation method and tool for assessing energy consumption in the building stock. Build. Environ. 75, 153–160. https://doi.org/10.1016/j.buildenv.2014.02.001.
UN-Habitat, 2010. A new chapter in urban development. Urban World. 2, p. 6.
Vinyes Ballbé, R., Molist Pujadas, L., Figueras Nart, M., 2018. De las formas de crecimiento a las formas del crecimiento. La caracterización morfológica de los tejidos metropolitanos residenciales de Barcelona. In: Monclús, J., Díez Medina, C. (Eds.), Ciudad y Formas Urbanas: Perspectivas Transversales. Volumen 3. Formas Urbanas y Regeneración Urbana. Prensas de la Universidad de Zaragoza e Institución Fernando el Católico, Zaragoza, pp. 197–207 https://doi.org/10.26574/uz.9788417358822.
Wiginton, L.K., Nguyen, H.T., Pearce, J.M., 2010. Quantifying rooftop solar photovoltaic potential for regional renewable energy policy. Comput. Environ. Urban. Syst. 34, 345–357. https://doi.org/10.1016/j.compenvurbsys.2010.01.001.
Wong, M.S., Zhu, R., Liu, Z., Lu, L., Peng, J., Tang, Z., Lo, C.H., Chan, W.K., 2016. Estimation of Hong Kong's solar energy potential using GIS and remote sensing technologies. Renew. Energy 99, 325–335. https://doi.org/10.1016/j.renene.2016.07.003.
World Urbanization Prospects: The 2018 Revision. https://doi.org/10.18356/b9e995fe-en.
Yuan, J., Farnham, C., Emura, K., Lu, S., 2016. A method to estimate the potential of rooftop photovoltaic power generation for a region. Urban Clim. 17, 1–19. https://doi.org/10.1016/j.uclim.2016.03.001.